



The Gaia Parallax Discrepancy for the Cluster Pismis 19 and Separating δ Scutis from Cepheids

Daniel Majaess¹ , Charles J. Bonatto² , David G. Turner³ , Roberto K. Saito⁴ , Dante Minniti^{5,6} , Christian Moni Bidin⁷ , Danilo González-Díaz^{7,8} , Javier Alonso-García^{9,10} , Giuseppe Bono^{11,12} , Vittorio F. Braga¹² , Maria G. Navarro¹² ,

Giovanni Carraro¹³ , and Matias Gomez⁵

¹ Mount Saint Vincent University, Halifax, Canada; Daniel.Majaess@msvu.ca

² Departamento de Astronomía, Universidade Federal do Rio Grande do Sul, CP 15051, RS, Porto Alegre 91501-970, Brazil

³ Saint Mary's University, Halifax, Canada

⁴ Departamento de Física, Universidade Federal de Santa Catarina, Trindade 88040-900, Florianópolis, Brazil

⁵ Instituto de Astrofísica, Dep. de Física y Astronomía, Facultad de Ciencias Exactas, Universidad Andres Bello, Av. Fernández Concha 700, Santiago, Chile

⁶ Vatican Observatory, Specola Vaticana, V-00120, Vatican City State, Vatican City

⁷ Instituto de Astronomía, Universidad Católica del Norte, Av. Angamos 0610, Antofagasta, Chile

⁸ Universidad de Antioquia, Calle 70 52-21, Medellín, Colombia

⁹ Centro de Astronomía, Universidad de Antofagasta, Av. Angamos 601, Antofagasta, Chile

¹⁰ Millennium Institute of Astrophysics, Nuncio Monseñor Sotero Sanz 100, Of. 104, Providencia, Santiago, Chile

¹¹ Department of Physics, Università di Roma Tor Vergata, via della Ricerca Scientifica 1, 00133, Rome, Italy

¹² INAF—Osservatorio Astronomico di Roma, Via di Frascati 33, 00078 Monte Porzio Catone, Italy

¹³ Dipartimento di Fisica e Astronomia “Galileo Galilei,” Università degli Studi di Padova, Vico Osservatorio 3, I-35122, Padova, Italy

Received 2024 December 9; revised 2025 January 25; accepted 2025 February 7; published 2025 March 27

Abstract

Pre-Gaia distances for the open cluster Pismis 19 disagree with Gaia parallaxes. A Two Micron All Sky Survey (2MASS) JK_s red clump distance was therefore established for Pismis 19 (2.90 ± 0.15 kpc), which reaffirms that zero-point corrections for Gaia are required. OGLE GD-CEP-1864 is confirmed as a member of Pismis 19 on the basis of DR3 proper motions and its 2MASS+Vista Variables in the Vía Láctea color-magnitude position near the tip of the turnoff. That 0.3 day variable star is likely a δ Scuti rather than a classical Cepheid. The case revealed a pertinent criterion to segregate those two populations in tandem with the break in the Wesenheit Leavitt Law ($\simeq 0.5$ day). Just shortward of that period discontinuity are δ Scutis, whereas beyond the break lie first overtone classical Cepheids mostly observed beyond the first crossing of the instability strip.

Unified Astronomy Thesaurus concepts: Variable stars (1761); Star clusters (1567)

Materials only available in the online version of record: data behind figure

1. Introduction

I. Soszyński et al. (2020) and V. Ripepi et al. (2023) classified OGLE GD-CEP-1864 as a 0.3 day first overtone classical Cepheid on the basis of OGLE and Gaia observations. Subsequently, V. Ripepi et al. (2023) and D. Majaess et al. (2024a) suggested OGLE GD-CEP-1864 could be a Cepheid member of Pismis 19. The putative case is enticing given OGLE GD-CEP-1864 may be the shortest-period cluster Cepheid, thereby providing a critical calibrator for Cepheid period-age relations (e.g., G. Bono et al. 2005; D. G. Turner 2012a; R. I. Anderson et al. 2016). Such Cepheids are likewise key to constraining the minimum mass sampled by the hot extent of the blue loop at a given chemical composition (e.g., G. Bono et al. 2000). More broadly, cluster Cepheids are important, owing to their use in assessing the validity of the Gaia zero-point and benchmarking the Planck Λ CDM value of H_0 (e.g., M. C. Reyes & R. I. Anderson 2023). However, W. L. Freedman et al. (2024, CCHP) cautioned that Cepheids produce nearer extragalactic distances than TRGB and JAGB stars, whereas A. G. Riess et al. (2024, SH₀ES) express a separate view.

The cluster parameters and variable star classification must be confirmed to exploit the connection between Pismis 19 and

OGLE GD-CEP-1864. Indeed, the distance to Pismis 19 is contested (Table 1). E. Poggio et al. (2021) relied on (E)DR3 to establish a distance to Pismis 19 of 3.5 kpc ($\pi = 0.282 \pm 0.061$ mas), while T. Cantat-Gaudin et al. (2020) utilized DR2 data to determine a parallax and color-magnitude diagram distance of 3.9 kpc ($\pi = 0.255 \pm 0.086$ mas) and 3.5 kpc, accordingly. Conversely, D. Majaess et al. (2012) summarized pre-Gaia distances that converged near 2.5 kpc. Specifically, A. E. Piatti et al. (1998), G. Carraro (2011), and D. Majaess et al. (2012) obtained cluster distances of 2.40 ± 0.88 kpc, 2.5 ± 0.5 kpc, and 2.40 ± 0.15 kpc, respectively. The results imply that the Gaia distance to Pismis 19 is too remote, and a correction is needed.

In this study, a near-infrared red clump distance is evaluated for Pismis 19 by drawing upon Two Micron All Sky Survey (2MASS) JHK_s photometry and Gaia proper motions (R. M. Cutri et al. 2003; Gaia Collaboration et al. 2023). Moreover, new Vista Variables in the Vía Láctea (VVV) photometry¹⁴ (R. K. Saito et al. 2012, J. Alonso-García et al. 2025, in preparation) is used in tandem with 2MASS to construct a color-magnitude diagram and clarify the evolutionary status of OGLE GD-CEP-1864. Infrared JHK_s data are used to reduce uncertainties stemming from the extinction law. For example, G. Carraro et al. (2013) noted that the optical ratio $A_V/E(B - V)$

Original content from this work may be used under the terms of the [Creative Commons Attribution 4.0 licence](#). Any further distribution of this work must maintain attribution to the author(s) and the title of the work, journal citation and DOI.

¹⁴ Near $K_s \sim 14.5$ magnitude, the formal VVV uncertainties can be approximately a tenth of those associated with 2MASS.

Table 1
Pismis 19 Distance

Reference	Method	d (kpc)
A. E. Piatti et al. (1998)	BVI_c	2.40 ± 0.88
G. Carraro (2011)	$UBVRI_c$	2.5 ± 0.5
D. Majaess et al. (2012)	JHK_s	2.40 ± 0.15
This work	RC	2.90 ± 0.15
T. Cantat-Gaudin et al. (2020)	DR2	3.9
E. Poggio et al. (2021)	EDR3	3.5

is anomalous toward Westerlund 2 (Carina; see also D. G. Turner 2012b), whereas extinction law variations are relatively less pronounced in the infrared (e.g., D. Majaess et al. 2016). The emerging results fostered pertinent constraints on Pismis 19 and OGLE GD-CEP-1864.

2. Analysis

2.1. Distance to Pismis 19

An inspection of Gaia DR3 astrometry within $0.^{\prime}5$ of the cluster center reveals clear overdensities (Figure 1; $n=75$). Members adhere to the following proper motion: $\mu_\alpha, \mu_\delta = -5.48 \pm 0.11, -3.37 \pm 0.12 \text{ mas yr}^{-1}$, where the uncertainty is the median absolute deviation (i.e., to reduce the impact of outliers). The parallax is $\pi = 0.31 \pm 0.06 \text{ mas}$ ($d \simeq 3.23 \text{ kpc}$) and places the cluster closer than the T. Cantat-Gaudin et al. (2020) estimate. The aforementioned sampling radius was imposed to mitigate field star contamination, and culling criteria were applied (e.g., RUWE < 2 , RPLx > 2). OGLE GD-CEP-1864 possesses a DR3 parallax of $\pi = 0.28 \pm 0.03 \text{ mas}$, and the proper motion data are $\mu_\alpha, \mu_\delta = -5.59 \pm 0.03, -3.30 \pm 0.04 \text{ mas yr}^{-1}$. Consequently, OGLE GD-CEP-1864 is a member of Pismis 19.

The Gaia radial velocity (RV) for OGLE GD-CEP-1864 is $-34.2 \pm 10.2 \text{ km s}^{-1}$, where the uncertainty is ostensibly large because of the star's variable nature. Expanding the search to $r = 2'$ reveals 34 stars with Gaia velocities. Half that sample remains after restricting the analysis to stars with astrometry compatible with cluster membership ($\pi, \mu_\alpha, \mu_\delta$) and applying 2σ clipping. That subsample of cluster members has a mean $RV = -30.5 \pm 0.9 \text{ km s}^{-1}$, which bolsters the association between OGLE GD-CEP-1864 and Pismis 19.

A Gaia-cleaned 2MASS color-magnitude diagram is shown as Figure 2 ($n=106$). Cluster members were identified by their astrometry within 2σ of the results derived above and were restricted to those stars which, for example, possess a 2MASS AAA quality flag. The sampling radius was expanded to $\simeq 2'$ to ensure adequate red clump statistics. The encircled red clump is readily discernible in the color-magnitude diagram (Figure 2) and is characterized by $K_s = 10.97 \pm 0.11$ and $J - K_s = 1.22 \pm 0.04$. Such findings, in concert with red clump absolute magnitudes and an extinction law (D. Majaess et al. 2011; D. Majaess et al. 2016), yield $d = 2.80 \pm 0.16 \text{ kpc}$. That determination stemmed from a Monte Carlo simulation that included uncertainties associated with each term. Employing the C. D. Laney et al. (2012) absolute magnitudes ($M_J = -0.984 \pm 0.014$, $M_{K_s} = -1.613 \pm 0.015$) results in $d = 2.90 \pm 0.15 \text{ kpc}$. The latter estimate is favored since the absolute magnitudes were determined by an independent research team (C. D. Laney et al. 2012).

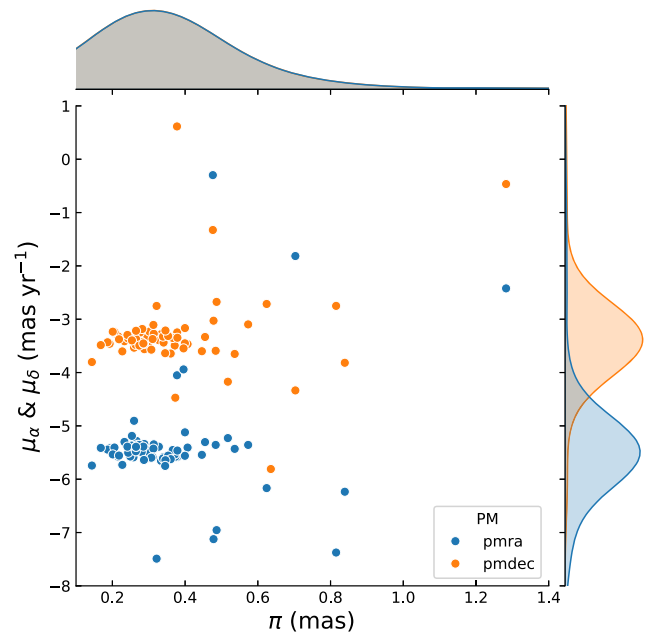


Figure 1. DR3 astrometry for stars within $\lesssim 0.^{\prime}5$ of the cluster center (Pismis 19). The overdensities represent probable cluster members (μ_α is blue, while μ_δ is orange).

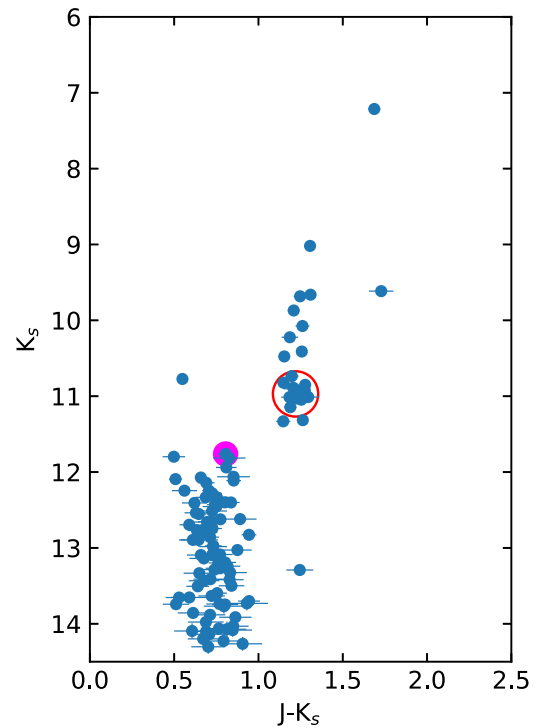


Figure 2. Probable cluster members (Gaia-cleaned) possessing AAA 2MASS photometry and uncertainties. The red clump stars are encompassed by a red circle. The magenta datum represents OGLE GD-CEP-1864.

An attempt was made to mitigate human bias, since a subset of the authors published distances for Pismis 19. The author R.K.S. pursued a separate derivation of the red clump distance and utilized the L. Ruiz-Dern et al. (2018) absolute magnitudes for red clump giants (i.e., $M_{K_s} = -1.605$, $(J - K_s)_o = 0.66$) and extinction laws from J. L. Sanders et al. (2022) and D. Minniti et al. (2018) ($A_{K_s}/E(J - K_s) = 0.448, 0.484$). Their determined distance supports the 2.9 kpc finding

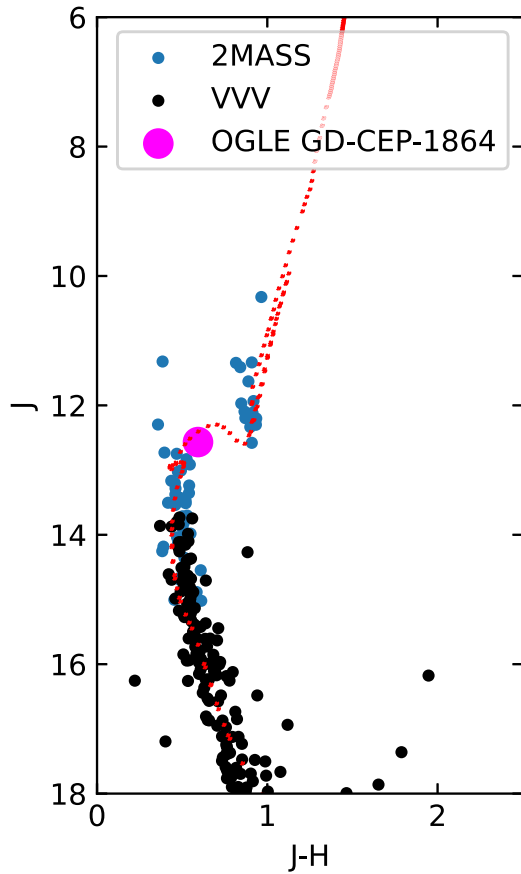


Figure 3. VVV (black, $r \lesssim 0.^{\circ}5$) + Gaia-cleaned 2MASS (blue, $r \lesssim 1.^{\circ}25$) color-magnitude diagram for stars along the Pismis 19 sight line. A solar isochrone ($\log \tau = 8.80 \pm 0.15$) was applied using parameters inferred from the cluster's red clump stars.

(The data used to create this figure are available in the [online article](#).)

($\mu_0 = 12.331 \pm 0.204$). Ideally, a preferable approach to reduce bias is a blind process (e.g., E. Chaussidon et al. 2025; W. L. Freedman et al. 2024, DESI and CCHP, accordingly).

The red clump distance, together with the pre-Gaia results, indicate that the DR3 parallaxes for Pismis 19 members are too small and a zero-point problem exists (e.g., L. Lindegren et al. 2021; K. A. Owens et al. 2022). Applying the L. Lindegren et al. (2021) correction to stars highlighted in Figure 2 revises the DR3 distance to $\simeq 3.1$ kpc. Alternatively, a weighted mean was derived employing the C. A. L. Bailer-Jones et al. (2021) approach (3.16 ± 0.10 kpc), which likewise relies on the L. Lindegren et al. (2021) correction.

A deeper color-magnitude diagram was constructed to unveil fainter Pismis 19 members sampled by new VVV photometry, thereby improving constraints on the evolutionary status of the cluster and OGLE GD-CEP-1864. The VVV stars were standardized to 2MASS using common stars in the field. A J versus $J - H$ diagram (Figure 3) was constructed using VVV ($r \lesssim 0.^{\circ}5$, $n = 146$) and Gaia-cleaned 2MASS ($r \lesssim 1.^{\circ}25$, $n = 55$) observations, whereby the former was a multi-epoch campaign, and the latter is generally a single-epoch survey. A Padova $\log \tau = 8.80 \pm 0.15$ scaled-solar isochrone was applied (see also B. Salasnich et al. 2000; C. Bonatto et al. 2004),¹⁵ namely by partly constraining

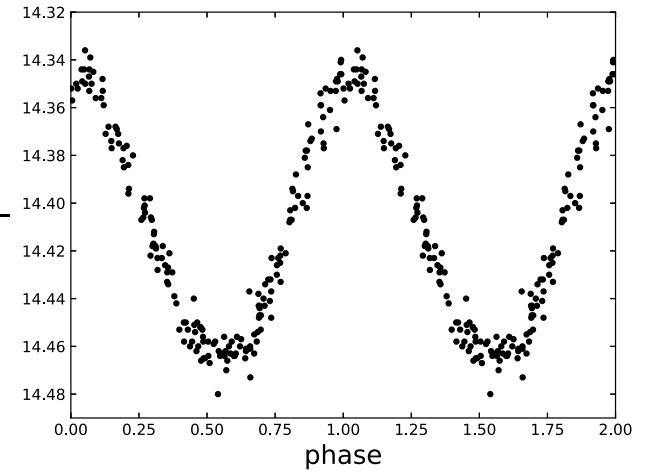


Figure 4. I -band light curve for OGLE GD-CEP-1864 from I. Soszyński et al. (2020). The data were repeated beyond phase > 1 .

Table 2
OGLE GD-CEP-1864 Parameters

P (day)	I	I_a	R_{21}	ϕ_{21}
0.2919180	14.407	0.118	0.089	3.982

Note. Variable star parameters stem from I. Soszyński et al. (2020), and the columns represent the pulsation period, mean I -band, I -band amplitude, and Fourier coefficients.

the degenerate sample space using red clump members. Specifically, the parameters utilized were $d = 2.9$ kpc and $E(J - H) = 0.40 \pm 0.02$ and rely on the D. Majaess et al. (2016) extinction laws and the C. D. Laney et al. (2012) red clump absolute magnitudes. OGLE GD-CEP-1864 lies near the tip of the turnoff (Figure 3). The author C.J.B. conducted a separate JK_s color-magnitude analysis following precepts outlined by C. Bonatto (2019) and established a comparable age of $\tau = 750 \pm 25$ Myr ($\log \tau = 8.87$) and nearer distance ($2.73^{+0.24}_{-0.02}$ kpc). The determinations overlap with the red clump results within the uncertainties.

2.2. OGLE GD-CEP-1864

OGLE GD-CEP-1864 was issued a preliminary classification on the basis of its light curve, which is conducive to a first overtone classical Cepheid (I. Soszyński et al. 2020; see also Figure 4 and Table 2). I. Soszyński et al. (2008) argued that first overtone classical Cepheids and δ Scutis obey the same Wesenheit Leavitt Law (T. G. Tsvetkov 1985; J. D. Fernie 1992), and adopted a convention whereby first overtone classical Cepheids exhibit $P \gtrsim 0.24$ day, and shortward of that period lie first overtone δ Scutis. Conversely, D. J. Majaess et al. (2011a) advocated that a break in slope is discernible near $\simeq 0.5$ day, which may differentiate the classes (their Figure 3, which was emphasized in part thanks to the new R. Poleski et al. 2010 δ Scuti photometry).¹⁶ I. Soszyński et al. (2023) revised their earlier interpretation after examining new observations and reaffirmed the aforementioned break near 0.5 day (bottom left panel of their Figure 5), while still favoring

¹⁵ $Z = 0.019$ was assumed; however, A. E. Piatti et al. (1998) suggest that Pismis 19 could instead be marginally subsolar.

¹⁶ Research by Bono and collaborators indicate the variables obey separate mass-luminosity relations (e.g., G. Bono et al. 1997).

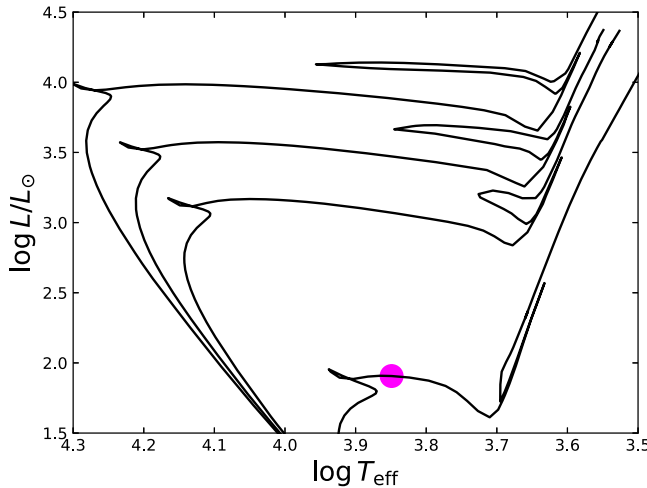


Figure 5. An H-R diagram hosting various isochrones ($\log \tau = 7.50, 7.75, 8.00, 8.80$) reaffirms that the blue loop does not extend to a sufficient temperature to sample OGLE GD-CEP-1864 (magenta). Scaled-solar Padova isochrones were utilized (see also B. Salasnich et al. 2000; C. Bonatto et al. 2004).

that first overtone δ Scutis possess $P \lesssim 0.23$ day (see also I. Soszyński et al. 2022). A separate interpretation is advocated here, namely that the division between the variable classes ($\simeq 0.5$ day rather than $\simeq 0.23$ day) is based on the period linked to the slope change and a notable shift in the principal crossing of the instability strip. First overtone δ Scutis are just prior to the period break, whereas beyond that threshold, first overtone classical Cepheids are primarily observed during later crossings of the instability strip. Importantly, V. Ripepi et al. (2022, their Figures 9 and 10) demonstrated a distinct shift longward of the slope divergence (0.58 ± 0.1 day) to blue loop crossings; however, they assumed variables near opposing sides of the break are all classical Cepheids (see also I. Soszyński et al. 2023). Figure 13 of G. Bono et al. (2024) contains a sample of OGLE-designated LMC classical Cepheids, and the later blue loop crossing does not extend to the temperatures of the faintest variables in their diagram (ostensibly δ Scutis), especially at solar metallicities (for broader discussions, see also H. Y. Xu & Y. Li 2004; G. Bono et al. 2005; D. G. Turner et al. 2006; R. I. Anderson et al. 2016).

In sum, the boundary between the classes could be set by the slope discontinuity and strip crossing. Figures 3 and 5 indicate OGLE GD-CEP-1864 is not sampled by a canonical blue loop, which in tandem with its position prior to the period associated with the diverging slope ($\simeq 0.5$ day) leads to a suggested reclassification as a δ Scuti variable.¹⁷ Shell hydrogen-burning first-crossing classical Cepheids are rare (e.g., Polaris, D. G. Turner 2009), and D. G. Turner et al. (2006, their Figure 4) argue the second and third crossings are dominant (longer) for Cepheids featuring $\log P \gtrsim +0.5$, whereas at lower periods, the fourth and fifth crossings are probable.

Lastly, for a first overtone δ Scuti, a Wesenheit Leavitt Law tied to OGLE VI LMC and Galactic photometry results in a distance of $\simeq 2.8$ kpc (relation from R. Poleski et al. 2010 and $\mu_{0,\text{LMC}}$ from I. Steer 2020). That matches the red clump finding; however, precise knowledge of shorter-wavelength extinction laws is especially important along this sight line

owing to sizable obscuration, hence the reliance on IR observations.

3. Conclusions

A new near-IR red clump distance for Pismis 19 reveals that DR3 parallaxes for cluster members are too small (Table 1) and possibly require a correction beyond the prescription detailed by L. Lindegren et al. (2021). OGLE GD-CEP-1864 is confirmed as a cluster member on the basis of astrometry (Figure 1) and its color-magnitude diagram position (Figure 3). OGLE GD-CEP-1864 (0.3 day) is suggested to be a δ Scuti variable (likely first overtone), rather than a classical Cepheid (Section 2.2). Importantly, the case reveals that those two variable classes may be distinguished by a change in the Wesenheit slope ($\simeq 0.5$ day) and their primary instability strip crossing.

Going forward, continued theoretical and asteroseismology research is desirable to better characterize δ Scuti pulsations in pre-main-sequence, main-sequence, and post-main-sequence stars (K. Zwintz et al. 2011; K. Zwintz 2017; J. A. Guzik 2021). Moreover, a dedicated characterization of other variable stars in the field may likewise provide pertinent context, and a period-change analysis for OGLE GD-CEP-1864 could confirm a positive period increase as indicated by Figure 5, assuming the variable is indeed beyond the earlier hotward Kelvin-Helmholtz phase. Regarding the cluster, a future aspect to examine is whether Pismis 19 exhibits evidence of tidal stripping by the Galactic field, especially given the cluster's age ($\log \tau = 8.80 \pm 0.15$, Figure 3). Examples include the broader field of NGC 6216 (D. Majaess et al. 2024a) and the open cluster triad of M25, NGC6716, Cr 394 (D. Majaess et al. 2024b).

Acknowledgments

The referee's suggestions to improve the manuscript were appreciated. This research relied on initiatives such as OGLE, VMC, IRSF, CDS, NASA ADS, arXiv, Gaia, Hipparcos, and VVV (data from the ESO Public Survey program IDs 179.B-2002 and 198.B-2004, taken with the VISTA telescope, and data products from the Cambridge Astronomical Survey Unit). D. Minniti gratefully acknowledges support from the Center for Astrophysics and Associated Technologies (CATA) by ANID BASAL projects ACE210002 and FB210003, and Fondecyt Project No. 1220724. R.K.S. acknowledges support from CNPq/Brazil through projects 308298/2022-5 and 421034/2023-8. G.B. and V.B. acknowledge support from project PRIN MUR 2022 (code 2022ARWP9C), “Early Formation and Evolution of Bulge and Halo (EFEBHO)” (PI: M. Marconi), funded by the European Union-Next Generation EU; and large grant INAF 2023 MOVIE (PI: M. Marconi).

ORCID iDs

- Daniel Majaess  <https://orcid.org/0000-0001-8803-3840>
- Charles J. Bonatto  <https://orcid.org/0000-0002-4102-1751>
- David G. Turner  <https://orcid.org/0000-0003-1184-1860>
- Roberto K. Saito  <https://orcid.org/0000-0001-6878-8648>
- Dante Minniti  <https://orcid.org/0000-0002-7064-099X>
- Christian Moni Bidin  <https://orcid.org/0009-0004-3783-6378>
- Danilo González-Díaz  <https://orcid.org/0000-0003-1698-4924>
- Javier Alonso-García  <https://orcid.org/0000-0003-3496-3772>
- Giuseppe Bono  <https://orcid.org/0000-0002-4896-8841>
- Vittorio F. Braga  <https://orcid.org/0000-0001-7511-2830>
- Maria G. Navarro  <https://orcid.org/0000-0002-1860-2304>

¹⁷ See also evolved δ Scutis in NGC 1817 (T. Arentoft et al. 2005; D. J. Majaess et al. 2011b, the latter's Figure 5) and NGC 1846 (R. Salinas et al. 2018, their Figure 6).

Giovanni Carraro <https://orcid.org/0000-0002-0155-9434>
 Matias Gomez <https://orcid.org/0000-0002-4430-9427>

References

- Anderson, R. I., Saio, H., Ekström, S., Georgy, C., & Meynet, G. 2016, *A&A*, **591**, A8
 Arentoft, T., Bouzid, M. Y., Sterken, C., Freyhammer, L. M., & Frandsen, S. 2005, *PASP*, **117**, 601
 Bailer-Jones, C. A. L., Rybizki, J., Fouesneau, M., Demleitner, M., & Andrae, R. 2021, *AJ*, **161**, 147
 Bonatto, C. 2019, *MNRAS*, **483**, 2758
 Bonatto, C., Bica, E., & Girardi, L. 2004, *A&A*, **415**, 571
 Bono, G., Braga, V. F., & Pietrinferni, A. 2024, *A&ARv*, **32**, 4
 Bono, G., Caputo, F., Cassisi, S., et al. 1997, *ApJ*, **477**, 346
 Bono, G., Caputo, F., Cassisi, S., et al. 2000, *ApJ*, **543**, 955
 Bono, G., Marconi, M., Cassisi, S., et al. 2005, *ApJ*, **621**, 966
 Cantat-Gaudin, T., Anders, F., Castro-Ginard, A., et al. 2020, *A&A*, **640**, A1
 Carraro, G. 2011, *A&A*, **536**, A101
 Carraro, G., Turner, D., Majaess, D., & Baume, G. 2013, *A&A*, **555**, A50
 Chaussidon, E., de Mattia, A., Yèche, C., et al. 2025, *JCAP*, **2025**, 135
 Cutri, R. M., Skrutskie, M. F., van Dyk, S., et al. 2003, *yCat*, **II/246**
 Fernie, J. D. 1992, *AJ*, **103**, 1647
 Freedman, W. L., Madore, B. F., Jang, I. S., et al. 2024, arXiv:2408.06153
 Gaia Collaboration, Vallenari, A., Brown, A. G. A., et al. 2023, *A&A*, **674**, A1
 Guzik, J. A. 2021, *FRASS*, **8**, 55
 Laney, C. D., Joner, M. D., & Pietrzynski, G. 2012, *MNRAS*, **419**, 1637
 Lindegren, L., Bastian, U., Biermann, M., et al. 2021, *A&A*, **649**, A4
 Majaess, D., Turner, D., Dékány, I., Minniti, D., & Gieren, W. 2016, *A&A*, **593**, A124
 Majaess, D., Turner, D., Moni Bidin, C., et al. 2011, *ApJL*, **741**, L27
 Majaess, D., Turner, D., Moni Bidin, C., et al. 2012, *A&A*, **537**, L4
 Majaess, D. J., Turner, D. G., Lane, D. J., Henden, A. A., & Krajci, T. 2011a, *JAVSO*, **39**, 122
 Majaess, D. J., Turner, D. G., Lane, D. J., & Krajci, T. 2011b, *JAVSO*, **39**, 219
 Majaess, D., Turner, D. G., Minniti, D., Alonso-Garcia, J., & Saito, R. K. 2024a, *PASP*, **136**, 094202
 Majaess, D., Turner, D. G., & Usenko, I. 2024b, *RNAAS*, **8**, 205
 Minniti, D., Saito, R. K., Gonzalez, O. A., et al. 2018, *A&A*, **616**, A26
 Owens, K. A., Freedman, W. L., Madore, B. F., & Lee, A. J. 2022, *ApJ*, **927**, 8
 Piatti, A. E., Clariá, J. J., Bica, E., Geisler, D., & Minniti, D. 1998, *AJ*, **116**, 801
 Poggio, E., Drimmel, R., Cantat-Gaudin, T., et al. 2021, *A&A*, **651**, A104
 Poleski, R., Soszyński, I., Udalski, A., et al. 2010, *AcA*, **60**, 1
 Reyes, M. C., & Anderson, R. I. 2023, *A&A*, **672**, A85
 Riess, A. G., Scolnic, D., Anand, G. S., et al. 2024, *ApJ*, **977**, 120
 Ripepi, V., Chemin, L., Molinaro, R., et al. 2022, *MNRAS*, **512**, 563
 Ripepi, V., Clementini, G., Molinaro, R., et al. 2023, *A&A*, **674**, A17
 Ruiz-Dern, L., Babusiaux, C., Arenou, F., Turon, C., & Lallement, R. 2018, *A&A*, **609**, A116
 Saito, R. K., Hempel, M., Minniti, D., et al. 2012, *A&A*, **537**, A107
 Salasnich, B., Girardi, L., Weiss, A., & Chiosi, C. 2000, *A&A*, **361**, 1023
 Salinas, R., Pajkos, M. A., Vivas, A. K., Strader, J., & Contreras Ramos, R. 2018, *AJ*, **155**, 183
 Sanders, J. L., Smith, L., González-Fernández, C., Lucas, P., & Minniti, D. 2022, *MNRAS*, **514**, 2407
 Soszyński, I., Pietrukowicz, P., Udalski, A., et al. 2023, *AcA*, **73**, 105
 Soszyński, I., Poleski, R., Udalski, A., et al. 2008, *AcA*, **58**, 163
 Soszyński, I., Udalski, A., Szymański, M. K., et al. 2020, *AcA*, **70**, 101
 Soszyński, I., Udalski, A., Skowron, J., et al. 2022, *AcA*, **72**, 245
 Steer, I. 2020, *AJ*, **160**, 199
 Tsvetkov, T. G. 1985, *Ap&SS*, **117**, 227
 Turner, D. G. 2009, in AIP Conf. Ser. 1170, Stellar Pulsation: Challenges for Theory and Observation, ed. J. A. Guzik & P. A. Bradley (Melville, NY: AIP), 59
 Turner, D. G. 2012a, *JAVSO*, **40**, 502
 Turner, D. G. 2012b, *Ap&SS*, **337**, 303
 Turner, D. G., Abdel-Sabour Abdel-Latif, M., & Berdnikov, L. N. 2006, *PASP*, **118**, 410
 Xu, H. Y., & Li, Y. 2004, *A&A*, **418**, 213
 Zwintz, K. 2017, in Second BRITE-Constellation Science Conf.: Small Satellites—Big Science, 5, ed. K. Zwintz & E. Poretti (Warsaw: Polish Astronomical Society), 228
 Zwintz, K., Lenz, P., Breger, M., et al. 2011, *A&A*, **533**, A133